CIVIL ENGINEERING JOURNAL

Article no. 8

THE CIVIL ENGINEERING JOURNAL 1-2023

FIELD EXPERIMENTAL STUDY ON EXTERNAL PRESTRESSING REINFORCEMENT OF A 420M PC CONTINUOUS BEAM BRIDGE

Sun Zhonglin, Sun Quansheng, Li Jianfei and Yang Shengqi

Department of Civil Engineering, Northeast Forestry University, Harbin， 150040, China; sunquansheng@nefu.edu.cn

ABSTRACT

In this paper, the practical engineering of a 420 m prestressed concrete （PC） continuous beam bridge is taken as the research object, and an external prestressing reinforcement method is proposed to reinforce the damaged and cracked girder. The paper is to study the structural performance of a PC continuous beam bridge before and after reinforcement. The heavy vehicle loading test of the reinforced PC continuous beam bridge was carried out. A total of three test spans were selected, and each test span selected seven deflection test sections and a strain test section. The corresponding finite element model was established and verified by the test results. Finally, it was concluded in this study that the external prestressing reinforcement method has a good effect on improving the loading capacity performance of damaged bridges.

KEYWORDS

External prestressing reinforcement, PC continuous beam bridge, Static load analysis, Finite element analysis

INTRODUCTION

Current status of research

In the late 20th century, many reinforced concrete bridges were built in China[1]. With the increase of traffic load and service time, there are also construction defects and environmental changes[2]~[3]. Many bridges have problems such as excessive mid-span deflection, cracking of beam bottom and web[4]. Reinforcement or replacement of old bridges is necessary to ensure safe operation of bridges. If the main beam is replaced directly, it will cause economic losses and vehicle traffic problems[5]. In order to effectively improve the loading capacity and service life of bridges. Many effective reinforcement methods are proposed and applied to the bridge reinforcement[6]~[9].

Before the reinforcement and maintenance of an old bridge, we should first examine and analyse the existing diseases of the old bridge itself, and then select an appropriate reinforcement measure according to the specific situation [10]. External prestressing is widely used to repair existing structures and build new bridges [11] to [14]. This study selected the most suitable external prestressing reinforcement method according to the specific engineering characteristics.

In order to study the performance of external prestressing reinforcement technology, the situation before and after external prestressing reinforcement is compared. The finite element analysis model of the whole bridge is established. The test results are compared with the calculation results of the finite element analysis model, and the performance of the external prestressing reinforcement technology is analysed and evaluated.

Defects of old bridge

A 420 m PC continuous girder bridge was completed in September 1995. Cracks appeared in the roof, floor, and web of the main girder of the bridge under long-term vehicle load and the surrounding environment. Overall, there were more cracks on the outer surface of the bridge. The majority of the crack width is concentrated in the range of 0.10 mm to 0.40 mm, and the length ranges from 0.3 m to 2.6 m. The width, length, and number of these cracks tend to increase over time. The bridge layout is shown in Figure 1.

(a) Field bridge

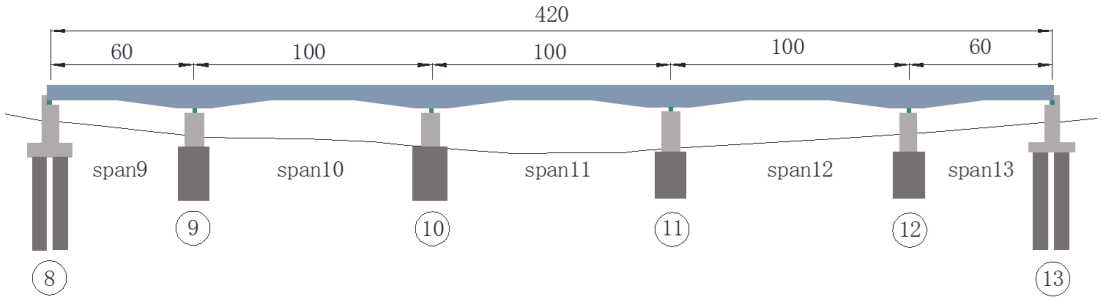

(b)Span and number

Fig.1 - Bridge type layout (unit：m)

At span 9, 5.49 m from the top of pier 9, inclined cracks began to appear on the web. Two oblique cracks were found. The crack lengths were 1 m and 0.91 m, respectively. The crack widths were 0.06 mm and 0.08 mm, respectively. The inclined cracks of spans 10, 11, and 12 were mostly concentrated between 34 and 39.5 meters from the fulcrum. The crack length was 0.41 m to 1.34 m. The crack width is 0.12 mm to 0.42 mm. They are caused by the principal tensile stress. Bending cracks appeared over a distance of 17.8 to 12.4 m. The crack height was between 0.06 m and 0.23 m. The crack width was between 0.02 mm and 0.14 mm. At span 13, 4.43 m from the top of pier 14, the web began to appear inclined. The crack length was 1.15 m. The crack width was 0.12 mm.

Secondly, the box girder floor and roof were checked. Some of the floor cracks were inclined cracks on both sides of the web extending to the middle line of the floor, while others were parallel to the bridge direction. The number of cracks increased gradually from each pier to the middle span. The number of floor cracks in span 10, span 11, and span 12 box girders increased gradually from the pier to the midspan direction. The two sides of the middle line of the floor cracks were symmetrical. In the range of 20 m on both sides of each pier, the bottom plate of the box girder had mainly longitudinal cracks. In the L/4 ~ 3L/4 section, a number of inclined cracks appeared in the bottom plate near the edge of the web. The floor crack width was mainly concentrated between 0.1 mm and 0.4 mm. The length of the crack was mostly concentrated in 0.70 m ~ 4.60 m. The roof

cracks were symmetrically distributed along the bridge deck midline and increased from the pier to the midspan direction. The longest crack was 5.34 m. The maximum crack width was 0.34 mm. In the range of 15.5 m from the piers on both sides (pier 10 and pier 11), dense intermittent longitudinal cracks appeared. The crack length was between 0.30 m and 2.60 m. The crack width was between 0.08 mm and 0.18 mm. The distribution of main cracks in box girders is shown in Figure 2. (Symbol description: crack length is expressed as *L=0.1m*, crack width is expressed as *δ=0.1mm*, crack tilt angle is expressed as *α=45°*)

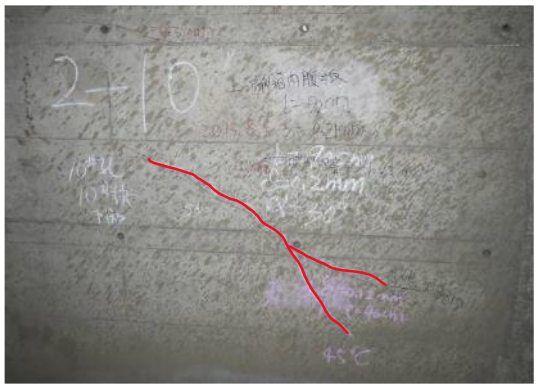

(a) Inclined cracks in the web near the roof of No.10 pier (L=0.9m δ=0.2mm α=45°)

(b) Inclined cracks of the web near the top of No.11 pier (L=2.2m δ=0.18mm α=45°)

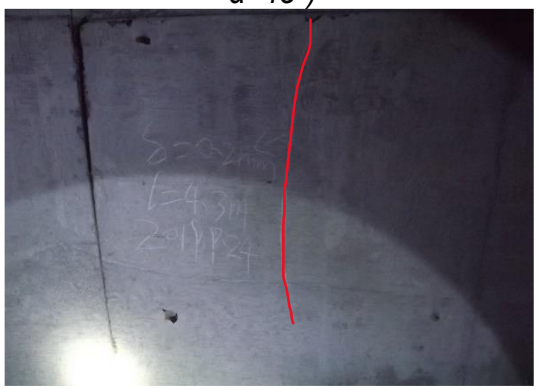

(c) Inclined cracks in the web near the top of No.9 pier (L=4.3m δ=0.2mm α=45°)

(d) Inclined cracks in the web near the top of No.13 pier (L=3.6m δ=0.1mm α=35°)

(e) Inclined cracks of the bottom plate in No.10 hole (L=4.4m δ=0.3mm α=45°)

(f) Inclined cracks of the bottom in No.12 hole (L=5.7m δ=0.4mm α=35°)

(i) Longitudinal cracks in the roof near of No.10 pier (L=2.5m δ=0.2mm α=15°)

(j) Longitudinal cracks in the roof near of No.11 pier (L=1.8m δ=0.3mm α=10°)

Fig.2 - Cracks distribution on the beam.

Finally, the crack distribution of the prestressed tooth plate and diaphragm was checked. There were many inclined cracks at the bottom of the roof at the top prestressed tooth plate of pier 9 and the top prestressed tooth plate of pier 14. The crack length was 0.15 m to 0.52 m. The crack width was 0.08 mm to 0.20 mm. The inclination angle was 30° ~ 60°. There were no stress cracks discovered in the diaphragms of piers 10, 11, 12, and 13. The diaphragm at the middle section of span 9 ~ 13 had vertical cracks on the top of the passing holes. On the one hand, the crack cracked horizontally downward along the direction of hole thickness. On the other hand, it extended vertically upward to the bottom of the roof. The width was between 0.14 mm and 0.30 mm. The length was between 0.35 m and 1.43 m. The distribution of specific cracks is shown in Figure 3.

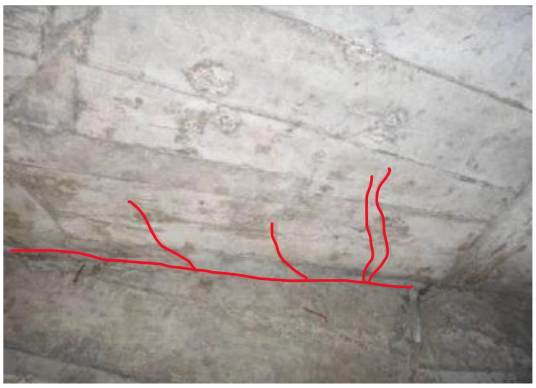

(a) Inclined cracks of tooth plate of No.11 box (L=0.52m δ=0.2mm)

(b) Cracks in diaphragm of No.12 box (L=1.43m δ=0.3mm)

Fig.3 - Crack distribution of tooth plate and diaphragm

Use a tape measure to determine the size of the crack. The crack tester measures the crack's width, and the cracks are categorized based on their placements. Classify all cracks examined as shown in Figure 4.

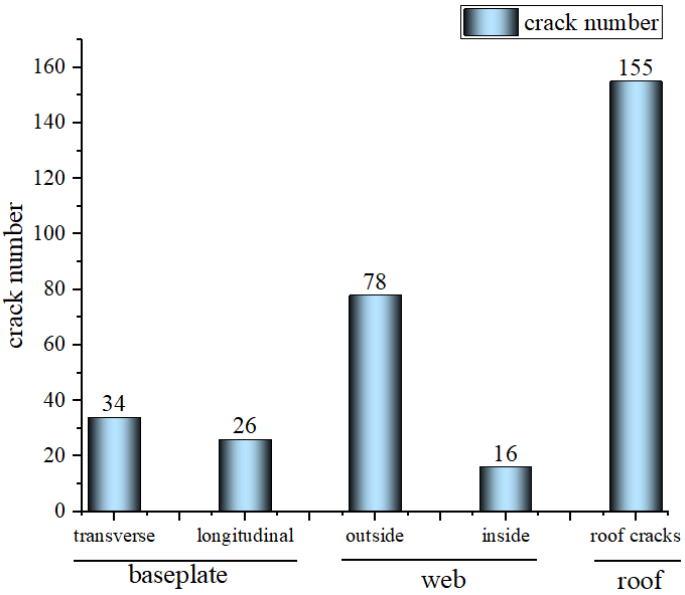

Fig.4 - Number of different types of cracks

METHODS

Layout of External Prestressed Steel Bundles

The externally prestressed tendons were added to the box girder to improve the cross-sectional strength, control the development of cross-section cracks, and effectively improve the stress of the girder. Six strands for span 9 and 13. Eight strands for span 10, 11 and 12, each consisting of 13 steel wires with a nominal diameter of 15.2 mm [15]. The two ends of the side span external prestressed steel beam were respectively anchored on the beam and the anchorage block. The middle-span external prestressed steel beam was cross-anchored on the anchorage block at the pier top. The detailed arrangement is shown in Figure 5.

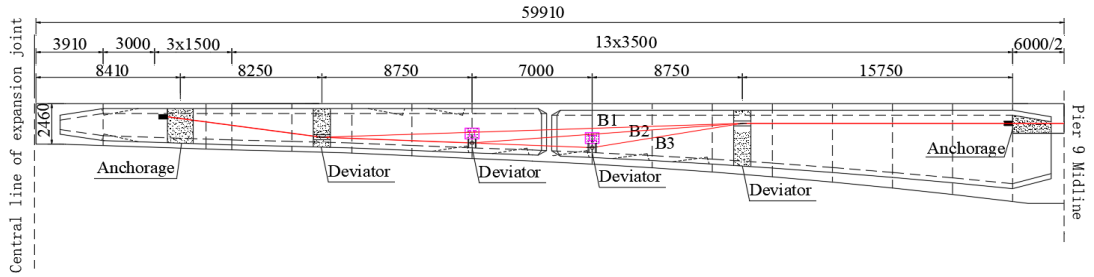

(a) span 9

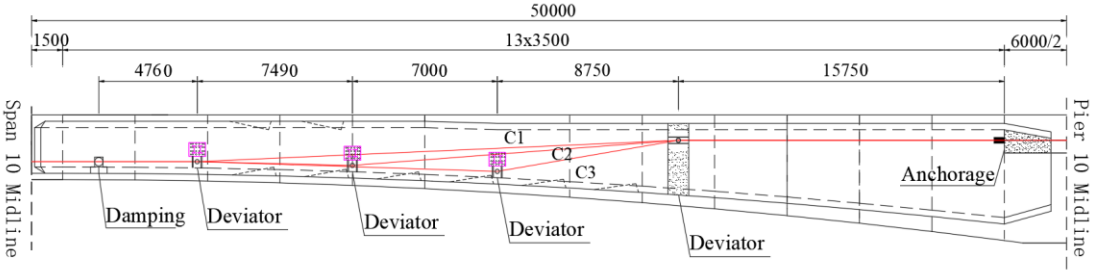

(b) span 10

Fig.5 - Detailed layout of steel beam（unit：mm）

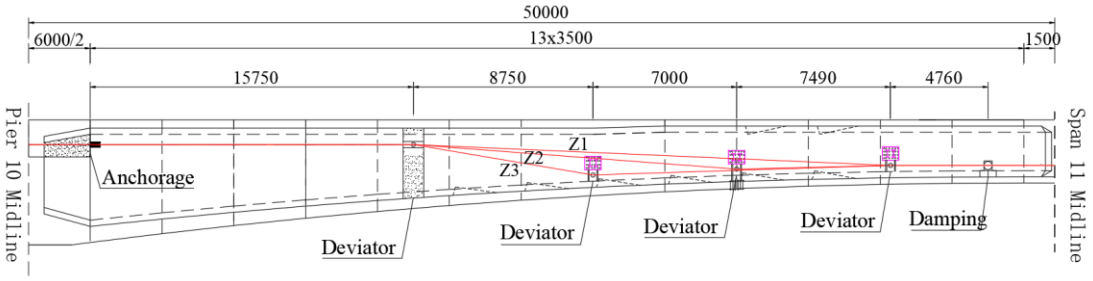

(c) span 11

Fig.5 - Detailed layout of steel beam（unit：mm）

The externally prestressed steel beam was tensioned at both ends. The tension control stress was 1209 MPa. The steel bundle was wrapped in a corrosion-resistant casing. Adjustable cable force and a replaceable anchor were used to facilitate future bridge maintenance. The field layout of externally prestressed tendons is shown in Figure 6.

Fig.6 - Field condition of external prestressed bundle

Test section and loading condition

This bridge's span combination was (60 + 3 x 100 + 60) m. Span 9, 10 and 11 were selected as the test spans. The control load was about 350 kN (according to Chinese design code JTG 021-1989[16]). Static load test using the principle of least favourable arrangement principle[17].The main test content was the deflection and strain of the test span. Finally, the structural performance parameters of the bridge before and after reinforcement were obtained.

Specific test sections were selected as follows: Seven deflection test sections and one strain test section were arranged for each span. The deflection test sections were located at L/8, 2L/8, 3L/8, 4L/8, 5L/8, 6L/8 and 7L/8. The strain test section was located at 4L/8. The specific layout is shown in Figure 7.

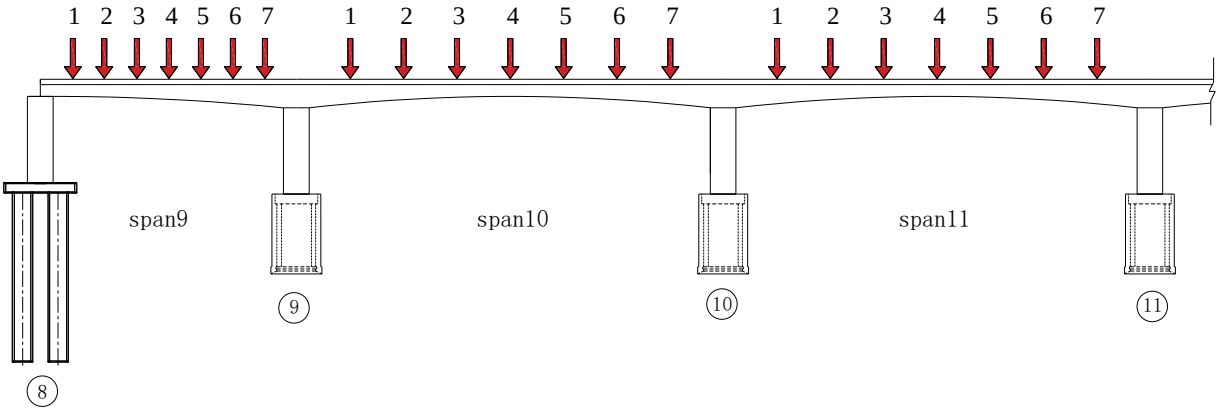

Fig.7 - Deflection and stress test sections

The static load test was divided into six conditions. Eight tri-axle trucks were used to simulate moving loads. A total weight of about 35 tons per truck. It takes 15 minutes to load each time. Then collect the data from each measuring point. Information about the loading condition is shown in Table 1. Loaded vehicle weight information is shown in Table 2. The loading vehicle arrangement is shown in Figure 8.

Tab. 1 - Test conditions and test items

Case No.	Location	Loading condition	Deflection Sensors	Strain Gauges
1	span 9 midspan	centric	√	√
2	span 10 midspan	centric	√	√
3	span 11 midspan	centric	√	√
4	span 9 midspan	eccentric	√	√
5	span 10 midspan	eccentric	√	√
6	span 11 midspan	eccentric	√	√

Tab. 2 - Characteristics of the loading truck (unit：kN)

Truck	Front axle	Middle axle	Rear axle	Total
1	70.1	140.1	140.1	350.3
2	70.2	140.5	140.5	351.2
3	69.9	140.6	140.6	351.1
4	70.4	140.5	140.5	351.4
5	70.2	140.4	140.4	351.0
6	70.3	140.2	140.2	350.7
7	70.3	140.2	140.2	350.7
8	70.4	140.3	140.3	351.0

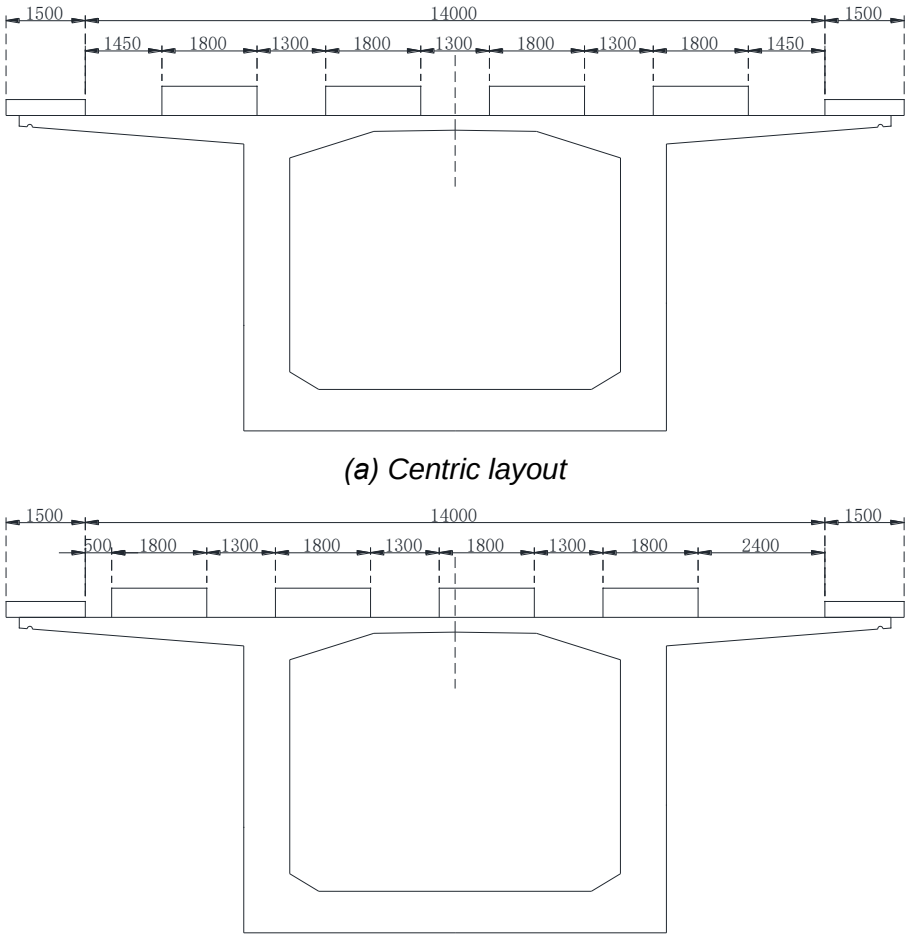

(a) Centric layout

(b) Eccentric layout

Fig.8 - Lateral arrangement of loaded vehicles (unit：mm)

The site vehicle arrangement is shown in Figure 9.

（a）Centric layout *（b）Eccentric layout*

Fig.9 - Site loaded vehicle arrangement

The strain sensors were arranged in the interior of the box girder. The measurement points were arranged on the top, web, and bottom surfaces at the mid-span position and on the top and web surfaces at the abutment position. The deflection was measured with a precision level. In deflection

measurement, the pier top was a fixed point. The tower ruler was placed on the test section. The precision level was placed on the pier top beam. The vertical deflection of the test section relative to the pier top was measured. The arrangement of measurement points is shown in Figure 10.

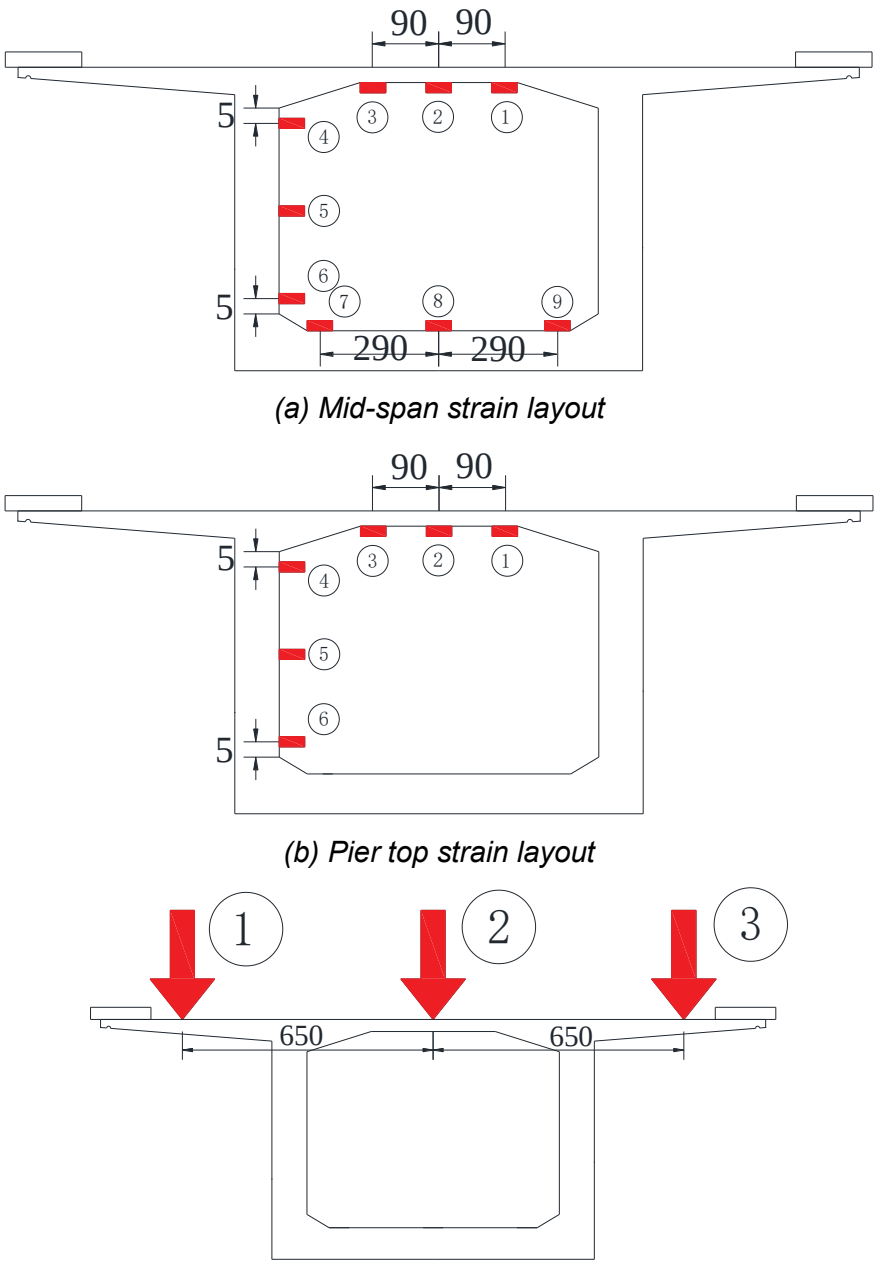

(a) Mid-span strain layout

(b) Pier top strain layout

(c) Deflection sensors layout

Fig.10 - Deflection and strain sensor locations illustration(unit：cm)

The picture of the field test is shown in Figure 11.

(a) Field measurement

(b) Field measurement

Fig.11 - Field measurement

RESULTS

Deflection

Deflection is an important parameter to characterize the bearing capacity of a bridge. The vertical deflection data and theoretical finite element model data of spans 9, 10 and 11 before and after reinforcement are shown in Figure 12.

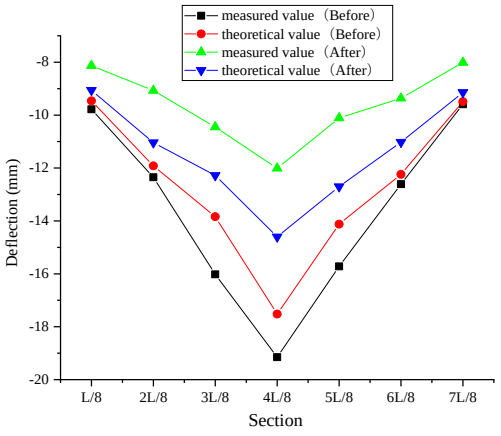

(a) Span 9 centric loadings

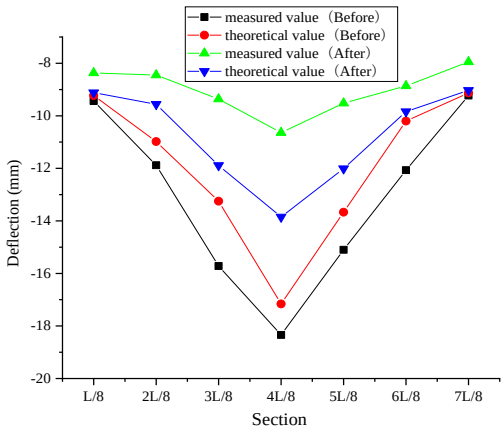

(b) Span 9 eccentric loading

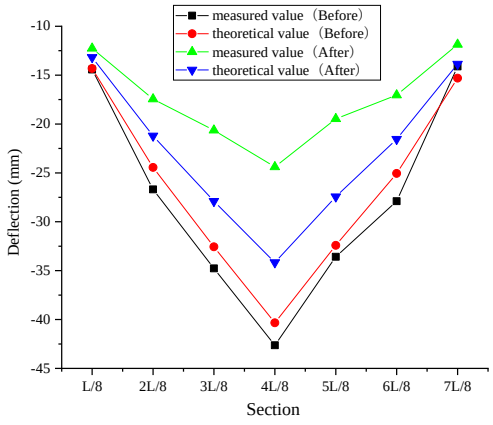

(c) Span 10 centric loadings

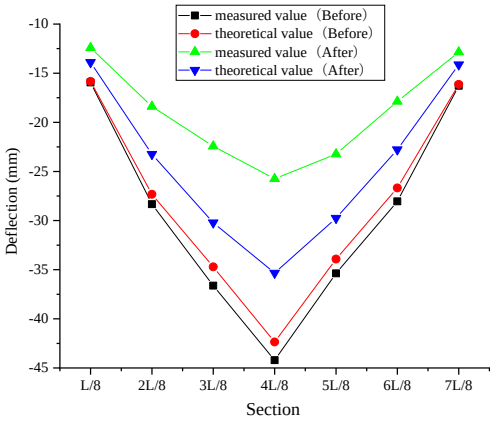

(d) Span 10 eccentric loading

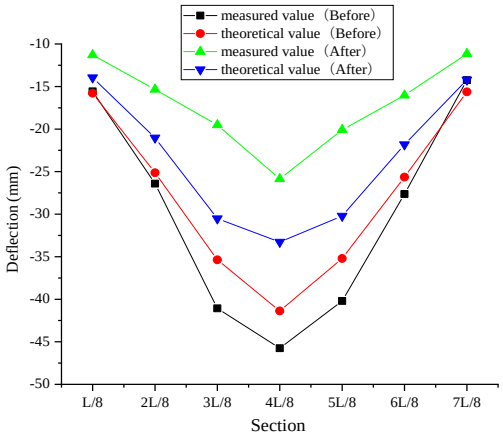

(e) span 11 centric loadings

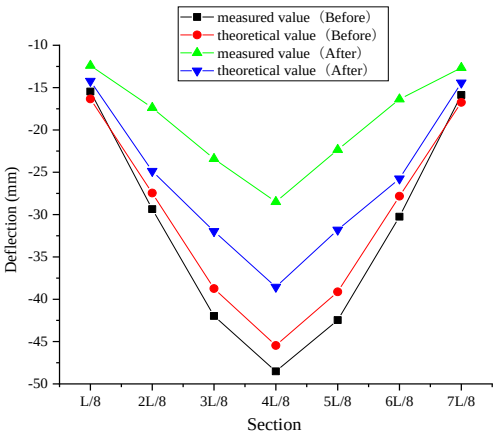

(f) Span 11 eccentric loading

Fig.12 - Vertical displacement data

According to the above curve, the bearing capacity of the No. 9 span increased by 18 %. The bearing capacity of the No. 10 span increased by 15%. The bearing capacity of No. 11 span increased by 18%. These results demonstrate how external prestress can greatly increase the structure's stiffness.

Comparison of deflection data before and after reinforcement. Most measured deflection data had exceeded theoretical data before reinforcement. After reinforcement, the measured deflection data has decreased to varying degrees. The maximum measured deflection after reinforcement is 28.49 mm, which is 41% lower than that before reinforcement of 48.52 mm.

Strain

Stress is another key data point reflecting bridge performance. The measured strain data before and after reinforcement and the theoretical data of the finite element model are shown in Figure 13.

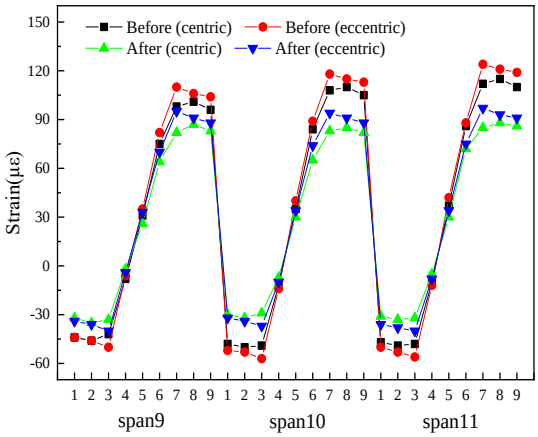

Fig.13 - Measured strain curve under static loading test

The overall performance of the three test spans improved after reinforcement. No. 9 span the strain calibration coefficient between 0.74 and 0.85, the average carrying capacity increased by 24 %, and the average calibration coefficient increased by 22 %. No. 10 span the strain calibration coefficient between 0.71 and 0.83, the average carrying capacity increased by 27 %, and the average calibration coefficient increased by 25 %. No. 11 span the strain calibration coefficient between 0.70 and 0.85, the average carrying capacity increasing by 26%, and the average calibration coefficient increasing by 23%.

From the loading position, the bearing capacity under the central loading condition is increased by 25% on average, and the verification coefficient is increased by 23% on average. Under eccentric loading, the bearing capacity is increased by 23%, and the calibration coefficient is increased by 24%.

At the top of pier 10, the bearing capacity increased by 14% on average. The calibration coefficient increased by 16% on average. The measured strain data are shown in Figure 14.

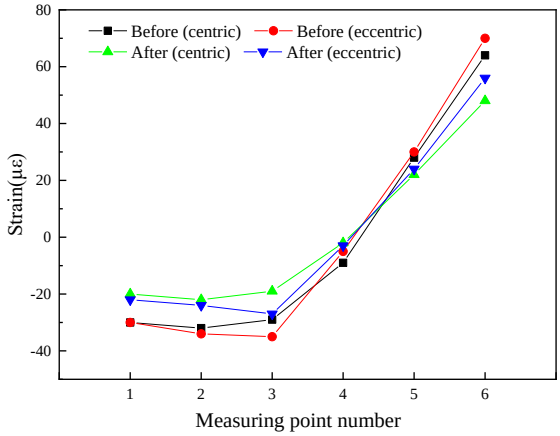

Fig.14 - Measured strain data under static loading test

After external prestressed reinforcement, the stiffness and bearing capacity of the bridge were significantly improved. The safety reserve of the bridge was increased. Which provides security for the continuous service of the bridge.

CONCLUSION

This paper describes the external prestressing reinforcement of a damaged PC continuous girder bridge. Then the static load tests of span 9, span 10, and span 11 are carried out. By comparing the measured data with the theoretical data of the finite element model. It is discovered that the bridge's overall performance has improved. The deflection and strain data after reinforcement are lower compared with those before reinforcement.

Overall, span 9, span 10, span 11 and pier 10 bearing capacity increased by 24%, 27%, 26%, and 14%, respectively. From the loading position analysis, the bearing capacity of central loading increased by 25% on average. The bearing capacity of eccentric loading increased by 23% on average. From the above data, the external prestressing reinforcement method proposed in this paper is very effective for improving the bearing capacity and overall performance of a PC continuous beam bridge with aging damage. In subsequent studies, the external prestressing reinforcement method can be applied to other types of old bridges or can be used in conjunction with some other reinforcement methods.

ACKNOWLEDGEMENTS

Funding: This work was supported by the Jilin Transportation Innovation Development Support (Science and Technology) Project [grant numbers 2020-1-9].

REFERENCES

[1] Editorial Department of China Highway Journal. (2014): Summary of academic research on bridge engineering in China. Journal of China Highway, Vol. 27(05), pp:1-96. DOI:10.19721/j.cnki.1001-7372.2014.05.001.

[2] Czaderski, C., Shahverdi, M., and Michels, J. (2021): Iron based shape memory alloys as shear reinforcement for bridge girders. Construction and building materials, Vol. 274, pp:121793. DOI:10.1016/j.conbuildmat.2020.

[3] Orta, L. (2013): Reliability Assessment of a Continuous Bridge Beam with Exposed Reinforcement. Engineering Structures, Vol. 262, pp:114281. DOI:10.1016/j.engstruct.2022.114281

[4] Editorial Department of China Highway Journal. (2021): Summary of academic research on bridge engineering in China. Journal of China Highway, Vol. 34(02), pp:1-97. DOI:10.19721/j.cnki.1001-7372.2021.02.001.

[5] Eamon, C. D., Jensen, E. A., Grace, N. F. (2012): Life-Cycle Cost Analysis of Alternative Reinforcement Materials for Bridge Superstructures Considering Cost and Maintenance Uncertainties. Journal of materials in civil engineering, vol. 24(4), pp:373-380. DOI:10.1061/(ASCE)MT.1943-5533.0000398.

[6] Michels, J., Staskiewicz, M., Czaderski, C., Kotynia, R., Harmanci, Y. E., and Motavalli, M. (2016): Prestressed CFRP Strips for Concrete Bridge Girder Retrofitting: Application and Static Loading Test. Journal of bridge engineering, vol. 21(5), pp: 4016003. DOI:10.1061/(ASCE)BE.1943-5592.0000835.

[7] Zhang, K., Sun, Q. (2018): Experimental Study of Reinforced Concrete T-Beams Strengthened with a Composite of Prestressed Steel Wire Ropes Embedded in Polyurethane Cement (PSWR-PUC). International journal of civil engineering, vol.16(9A), pp: 1109-1123. DOI:10.1007/s40999-017-0264-x.

[8] Jawdhari, A., Peiris, A., and Harik, I. (2018): Experimental study on RC beams strengthened with CFRP rod panels. Engineering structures, Vol. 173, pp: 693-705. DOI:10.1016/j.engstruct.2018.06.105.

[9] Cadenazzi, T., Dotelli, G., Rossini, M., Nolan, S., and Nanni, A. (2020): Cost and environmental analyses of reinforcement alternatives for a concrete bridge. Structure and infrastructure engineering, Vol. 16(4), pp: 787-802. DOI:10.1080/15732479.2019.1662066.

[10] Buchin-Roulie, V., Kaczkowski, N., Courcelles, C. D., and Toth, M. (2017): Innovative solution for bridge strengthening (for widening and compliance to new codes) by modification of initial static scheme. Paper presented at the IABSE Symposium, Vol. 2017, pp:2504-2511. DOI:10.2749/vancouver.2017.2504.

[11] Aparicio, A. C., Ramos, G., and Casas, J. R. (2002): Testing of externally prestressed concrete beams. Engineering structures, Vol. 24(1), pp: 73-84. DOI:10.1016/S0141-0296(01)00062-1.

[12] Tan, K. H., Tjandra, R. A. (2007): Strengthening of RC continuous beams by external prestressing. Journal of structural engineering-asce, Vol. 133(2), pp: 195-204. DOI:10.1061/(ASCE)0733-

9445(2007)133:2(195).
[13] Xu, J. L., Yi, Z. L., Yang, J. J. (2013): A Study on the Quality Assessment System of External Prestressing Reinforcement Technology. Applied Mechanics & Materials, Vol. 351-352, pp:1347-1353. DOI:10.4028/www.scientific.net/AMM.351-352.1347
[14] Shen, Y., Song, T., Li, G. (2015): Advances of external prestressing tendons in multi-span curved box-girder bridges: Multi-Span Large Bridges (pp: 1255-1262). DOI:10.1201/b18567-164
[15] JTG 3362-2018 Specifications for design of highway reinforced concrete and prestressed concrete bridges and culverts [S]. P.R. China, Ministry of Communications, 2018.
[16] JTJ 021-1989. General Code for Design of Highway Bridges and Culverts[S], P.R. China, Ministry of Communications,1989.
[17] JTG/T J21-01-2015 Load test methods for highway bridges [S]. P.R. China, Ministry of Communications, 2015.